ORIGINAL PAPER

Performance verification of different advanced oxidation processes in the degradation of the dye acid violet 17: reaction kinetics, toxicity and degradation prediction by artificial neural networks

Nathália F. S. de Moraes[1] · Rayany M. R. Santana[1] · Rayssa K. M. Gomes[1] · Sérgio G. Santos Júnior[1] ·
Alex L. A. de Lucena[1] · Léa E. M. C. Zaidan[1] · Daniella C. Napoleão[1]

Abstract

The contamination of water resources due to the presence of persistent organic pollutants, such as dyes, is a cause for concern, since these substances are resistant to conventional treatments adopted in wastewater treatment plants. In this context, the present work evaluated the degradation of the dye AV17, used in sanitizing industries, through different advanced oxidation processes (AOP). AOP of photoperoxidation, Fenton and photo-Fenton were employed. It was found that the photoperoxidation/UV-C system was more efficient in the treatment of the dye, reaching degradations of 68.27%, 88.16% and 99.35% for the characteristic wavelengths of 254, 307, 548 nm, respectively. The Fenton process and the photo-Fenton/solar system, especially with natural solar irradiation, only managed to promote the discoloration of the solution by degrading the chromophore group. The kinetic study indicated a better adjustment of the experimental data to the pseudo-first order model, with $R^2 > 0.94$ for the mentioned AOP. The modeling by ANN allowed to predict the degradation of AV17 through an MLP 5-6-3 BFGS 297 type network, with R^2 values higher than 0.9864 for training, testing and validation. Toxicity tests with *Lactuca sativa* seeds showed that the treatment via photoperoxidation/UV-C and photo-Fenton/solar led to a reduction in the toxicity of the solution contaminated by the dye. However, for the solution treated by Fenton process, toxicity was observed.

Keywords Degradation · *Lactuca sativa* · Mathematical modeling · Water

Introduction

The growing development and expansion of the industrial sector in the last decades are factors that concern the world scientific community regarding environmental issues. If, on the one hand, this growth has promoted an improvement in the quality of life of the population, on the other hand it is responsible for the high production of tailings, especially through the disposal of industrial effluents (Kumar et al. 2019). These effluents are complex matrices, whose composition is rich in persistent organic pollutants (POP),

which are difficult to remove through conventional physical–chemical and biological treatments (Brillas 2020; Ertugay and Acar 2017). Therefore, studies have been carried out to develop viable and effective technologies for the treatment of such waste, to minimize the environmental impacts caused to aquatic bodies (Brillas 2020; Korpe et al. 2019, Pavithra and Jaikumar 2019).

Textile, food and cosmetics industries stand out for the generation of effluents contaminated by chemical dyes, applied in their production process (Pavithra and Jaikumar 2019). The presence of these compounds in water bodies causes several environmental damages, due to the high toxicity (Jain and Gogate 2017), carcinogenic/mutagenic effect (Navarro et al. 2017, Golka et al. 2004) and low biodegradability (Martins, Rossi and Quinta-Ferreira 2010). In addition, these substances impart color to the water bodies, causing damage to the photosynthetic activity of the environment (Jain and Gogate 2017).

In this context, the advanced oxidation processes (AOP) have been consolidated as POP treatment technology, like

✉ Daniella C. Napoleão
daniella.napoleao@ufpe.br

[1] Universidade Federal de Pernambuco, Recife, PE 50740-521, Brazil

dyes, especially textiles (Ramos et al. 2020; Paździor et al. 2019; Kumar et al. 2019; Santana et al. 2019a, b) and food (Júnior et al. 2019; Santos et al. 2019; Álvarez et al. 2011). However, little has been said about its application for the degradation of dyes aimed at the sanitizing industry. In this industrial branch, household cleaning products are manufactured, such as bleach, detergents and soaps, which contain coloring substances in their formulation, as defined by the Brazilian Health Regulatory Agency (Brasil 2019). Thus, the industrial effluents discarded by this type of industry also deserve attention regarding the presence of such compounds.

For degradation of these compounds, the AOP use highly reactive radicals, such as hydroxyl radicals, obtained from oxidizing agents, such as ozone (O_3) and hydrogen peroxide (H_2O_2) (Elkacmi and Bennajah 2019). Obtaining these radicals is often promoted by the presence of ultraviolet (UV) and visible radiation (Pavithra and Jaikumar 2019). The use of radiation associated with the oxidizing agent has generated better degradation results, when compared to the isolated photolysis technique, as observed by Elkacmi and Bennajah (2019).

When these hydroxyl radicals are obtained from the decomposition of H_2O_2 in the presence of radiation, the process is called photoperoxidation (Utzig et al. 2019). Among the most used AOP there is the Fenton reaction, whose action of the oxidizing agent occurs under Fe^{+2} ion catalysis, obtained from ferrous salts, and under acidic conditions (Lastre-Acosta 2019). This process has some advantages, such as not requiring a radiation source for the activation of the oxidizing agent (Kumar et al. 2020a, b). The Fenton process can be photo-assisted, being then called photo-Fenton. The combined use of Fenton's reagents with radiation has often led to better degradation results as observed by Kumar et al. (2020a, b), Santana et al. (2017) and Abo-Farha (2010).

Despite aiming at the complete reduction of POP to CO_2, water and inorganic salts, AOP can also lead to the formation of intermediates whose toxicity may be higher than that of the original compounds (Fernandes et al. 2018; Nascimento et al. 2018; Ferrando-Climent et al. 2017; Stalter et al. 2010). Thus, it is necessary to assess the toxicity of the solutions that undergo these treatments. Some authors have carried out this analysis through the use of seeds, adopted as bioindicators, since it is a sensitive, simple and low-cost technique (Santana et al. 2019; Utzig et al. 2019).

In addition, the different AOP can also be studied in terms of reaction kinetics, to obtain a better understanding of the functioning of the process as a whole. The successive chemical reactions that comprise these processes present behavior that can be evaluated through previously developed models. These models present the degradation kinetics as a function of variables such as concentration of the degraded compound, pH, dosage of oxidizing agent and catalyst (Chan and Chu 2003). The degradation of

organic compounds by AOP follows, in general terms, a nonlinear model of pseudo-first order, but first and second order linear models are also applied, since they present good adjustment to experimental data (Santana et al. 2019b).

In addition to the kinetic study, the experimental data can also be adjusted through the use of empirical mathematical models, such as the artificial neural networks (ANN). ANN modeling uses the experimental data to make predictions regarding the efficiency of the process (Baştürk and Alver 2019; Charamba et al. 2018). Its application in the study of the degradation of organic pollutants by AOP has proved to be useful, in particular due to the complexity of the parameters that influence these processes (Monteiro et al. 2018).

Given the above, the present study aimed to evaluate the efficiency of photoperoxidation, Fenton and photo-Fenton AOP in the degradation of the acid violet 17 (AV17) in aqueous solution, under different radiation sources. The degradation kinetic of the dye was also evaluated, verifying the suitability of the experimental data from the process to kinetic models. In addition, simulations using artificial neural networks (ANN) were also carried out to establish a type of network capable of predicting the degradation of the dye under different conditions. Finally, the toxicity of the solution was evaluated before and after treatment.

Experimental

Identification and quantification of the acid violet 17 dye

For the study of the degradation of acid violet 17 (AV17), a working solution was prepared with a concentration of 20 mg L^{-1} of the compound. Abid et al. (2012) determined the concentration of dyes in a real effluent as being in the range of 20–50 mg L^{-1}. In textile effluents, these values are reported over a wide range, with variations from 10 to 800 mg L^{-1} (Yaseen and Sholz 2019). Considering that the dye under study comes from sanitizing industries, in which there is less use of these substances, the value adopted as the initial concentration (20 mg L^{-1}) is representative.

A spectral scan by ultraviolet/visible spectrophotometry (Thermoscientific, Genesys 10S model) was performed, to determine the characteristic wavelengths (λ) for the dye, for which the degradation was monitored. From this, analytical curves were constructed, with a linear range of 1 to 100 mg L^{-1}. For each of the curves, the values of the correlation coefficients of the analytical curves were determined (r) and the coefficient of variation (CV) was calculated, all according to the National Institute of Metrology Standardization and Industrial Quality (INMETRO 2016).

Preliminary study of advanced oxidative processes for dye degradation

The working solution was subjected to a preliminary study whose objective was to define the most efficient AOP for the degradation of the dye. For such, 50 mL of this solution were subjected to photoperoxidation, Fenton and photo-Fenton treatments, for a period of 60 min. In all processes, a concentration of hydrogen peroxide (35% Scientific Exodus), of 100 mg L^{-1} was used. For the Fenton and photo-Fenton processes, a concentration of iron ([Fe]) of 5 mg L^{-1} was applied, obtained from $FeSO_4 \cdot 7H_2O$ (Vetec) and the pH was adjusted to the 3–4 range, considered the optimum pH range to the Fenton reaction (Deshannavar et al. 2020), from a H_2SO_4 0.1 mol L^{-1} solution. Santana et al. (2019) also observed that this pH range is ideal for the degradation of textile dyes by the Fenton process.

In this study, the influence of the radiation source was also evaluated, for the photoperoxidation and photo-Fenton processes, using bench reactors equipped with UV-A and UV-C radiations, described by Charamba et al. (2018) and Zaidan et al. (2017), respectively, as well as one equipped with sunlight radiation (Santana et al. 2017). The luminous intensity inside the reactors was measured with the aid of a radiometer (Empórionet), with the values been of: 1.82×10^{-4} W cm^{-2} (UV-A) and 1.42×10^5 W cm^{-2} (UV-C). As regarding the sunlight reactor, the photo emission was 8.96×10^{-4} W cm^{-2} in the UV-A range, 5.90×10^{-3} W cm^{-2} in the UV-B range and 13.8 W cm^{-2} in the visible light range.

Optimization of working conditions

After defining the most efficient treatments, the best operating conditions were determined for each case. To this end, a univariate study of the $[H_2O_2]$ was done, varying it by: 40, 50, 60, 70, 80, 90 and 100 mg L^{-1}.

The Fenton process, without the use of radiation, had its operational conditions optimized by carrying out a factorial design (FD) 2^3 with a central point in triplicate. The variables evaluated for this process were: [Fe], $[H_2O_2]$ and pH. The levels adopted as minimum, central and maximum for these parameters were 1, 3 and 5 mg L^{-1}; 40, 80 and 120 mg L^{-1} and 2, 3 and 4, respectively. The constructions of the Pareto chart and the response surface were made using the *Statistica 6.0* software. The answer used to evaluate the efficiency of the processes was the percentage of degradation in each of the characteristic λ, with the exception of the FD in which the chromophore group was monitored only. All tests were conducted for 60 min.

Kinetic study of the degradation of the dye AV17 and determination of the residual H_2O_2

After determining the best working conditions for the most efficient processes, tests were carried out to monitor the degradation kinetics of the AV17 dye. For this, 1L of the working solution was submitted to each of the selected treatments, with 3 mL aliquots being removed at 0, 5, 10, 15, 20, 25, 30, 40, 50, 60, 90 and 120 min. The data obtained were interpreted according to the linear kinetic models of first and second order, described in Eqs. 1 and 2, respectively (Santana et al. 2019b).

$$\ln\left(\frac{C}{C_0}\right) = -k_1 t \tag{1}$$

$$\frac{1}{C} = \frac{1}{C_0} + k_2 \cdot t \tag{2}$$

where k_1 and k_2 are the kinetic constants of the respective models; C (mg.L^{-1}) is the concentration of the pollutant at a given time t (min); and C_0 (mg L^{-1}) is the initial concentration of the pollutant in the solution. The nonlinear kinetic model of pseudo-first order proposed by Chan and Chu (2003) was also tested (Eq. 3).

$$\frac{C}{C_0} = 1 - \frac{t}{\rho + \sigma t} \tag{3}$$

In this model, $\frac{1}{\rho}$ (min^{-1}) and $\frac{1}{\sigma}$ (dimensionless) represent the kinetic constant and the oxidative capacity of the system, respectively. After the experiments for the kinetic study, an additional analysis of the residual hydrogen peroxide concentration in the solution was performed. This was determined by the colorimetric method, using test strips of H_2O_2 (Merck), in the range of 0 to 25 mg L^{-1}.

Artificial neural network modeling

The mathematical modeling applying artificial neural networks (ANN) was simulated to predict the degradation of the AV17 dye, in three different λ, (254, 307, 548 nm), with the output parameters being the percentage of degradation in each one of these λ. The following parameters were used as input parameters for the tested ANN: [Fe], pH, $[H_2O_2]$, time and photon emission. To build the ANN, a multilayer percepton (MLP) configuration was used, the propagation signal being carried out through the neurons distributed in it, as well as in the hidden layer and its output. The sampling method was randomized with data divided into 70%, 15% and 15% for training, testing and validation, respectively. The ANN was trained using 200 iterations and 10 repetitions, totaling 2000 iterations. The

data obtained for the different networks evaluated were analyzed based on the values of the linear regression coefficients (R^2) and their errors for both training, testing and validation.

Toxicity tests using seeds

The evaluation of seed toxicity was made based on the methodology proposed by Santos et al. (2019). For this, lettuce seeds (*Lactuca sativa*) were exposed to the working solution before and after treatments, for an incubation period of 120 h, in the absence of light and at a temperature of 25 ± 1 °C. The tests were performed by placing 20 seeds in Petri dishes, using filter paper as a support. For each test, 4 mL of the mentioned solutions were used, as well as the negative (distilled water) and positive (3% boric acid solution) controls. All analyzes were performed in triplicate.

After the incubation period, the germinated seeds were counted and the root growth was measured to calculate the relative growth index (RGI) and the germination index (GI), as determined based on Eqs. 4 and 5.

$$RGI = \frac{RLS}{RLC} \tag{4}$$

$$GI(\%) = \frac{RLS \times GSS \times 100}{RLC \times GSC} \tag{5}$$

where RLS corresponds to the total length of the root in the sample; RLC, to the total length in the control; GSS, the number of seeds germinated in the sample; and GSC, the number of seeds germinated in the negative control (Young et al. 2012).

Results and discussion

Identification and quantification of the AV17 dye

After spectral scanning, from 200 to 700 nm, using the ultraviolet/visible (UV/Vis) spectrophotometry technique, it was possible to obtain the spectrum for the dye AV17 (Supplementary material). The characteristics wavelengths (λ) of 254 and 307 nm (auxochromes), and 548 nm (chromophore groups) were identified. Therefore, for each of these λ analytical curves were constructed, which showed good linearity, with Pearson correlation coefficients (r) greater than 0.99 (INMETRO 2016). In addition, it was found that the method used is accurate, since it presented a coefficient of variance value of less than 5% (Brasil 2003), for all λ analyzed.

Preliminary study of advanced oxidation processes for dye degradation

With the methodology for the identification and quantification of the dye under study, next step was testing the degradation of the AV17 dye. The results obtained for the preliminary study to evaluate the efficiency of the photolysis process, as well as the photoperoxidation AOP, Fenton and photo-Fenton, are shown in Table 1.

From the results presented in Table 1, it is possible to state that the photolysis process did not show good results for any of the radiation used, leading to low or no degradation of the AV17 for all λ under study. As described by Elkacmi and Bennajah (2019), the isolate use of radiation without association with oxidizing agents, has been shown to be inefficient in the degradation of persistent organic pollutants.

For photoperoxidation and photo-Fenton AOP, it appears that the use of UV-C radiation led to the best results, with degradation being observed for all λ monitored. Among the AOP, the photoperoxidation process deserves to be highlighted, promoting a high degradation of the chromophore group, as well as of the group observed at 307 nm, in addition to a partial degradation of the group observed at 254 nm. The photo-Fenton AOP using sunlight radiation promoted 100% degradation of the chromophore group under the applied conditions. However, this type of treatment was not able to degrade auxochromes. With regard to the Fenton process, it was also able to degrade the chromophore group, being, therefore, satisfactory only for the process of discoloration of the AV17, since it was inefficient for the other λ evaluated. The use of UV-A radiation did not lead to good results for any of the studied AOP. This behavior may be due to the fact that the production of hydroxyl radicals by decomposition of H_2O_2 occurs mainly in the range 200

Table 1 Preliminary study to evaluate the efficiency of the AOP in the degradation of dye AV17

AOP	Radiation	Degradation (%)		
		254 nm	307 nm	548 nm
Photolysis	UV-A	ND	ND	ND
	UV-C	**ND**	**ND**	**9.62 ± 2.02**
	Sunlight	ND	ND	ND
Photo-peroxidation	UV-A	ND	ND	ND
	UV-C	**65.88 ± 3.63**	**98.81 ± 0.12**	**99.55 ± 0.07**
	Sunlight	ND	30.53 ± 4.88	68.46 ± 6.96
Fenton	–	ND	ND	99.25 ± 0.01
Photo-Fenton	UV-A	ND	ND	96.30 ± 0.08
	UV-C	**16.97 ± 1.94**	**16.80 ± 0.99**	**97.17 ± 3.92**
	Sunlight	ND	1.69 ± 3.66	100.00

ND no degradation

to 300 nm, lower than the range of λ corresponding to UV-A radiation, which would explain the inefficiency observed for the submitted AOP to this radiation (Araújo et al. 2016).
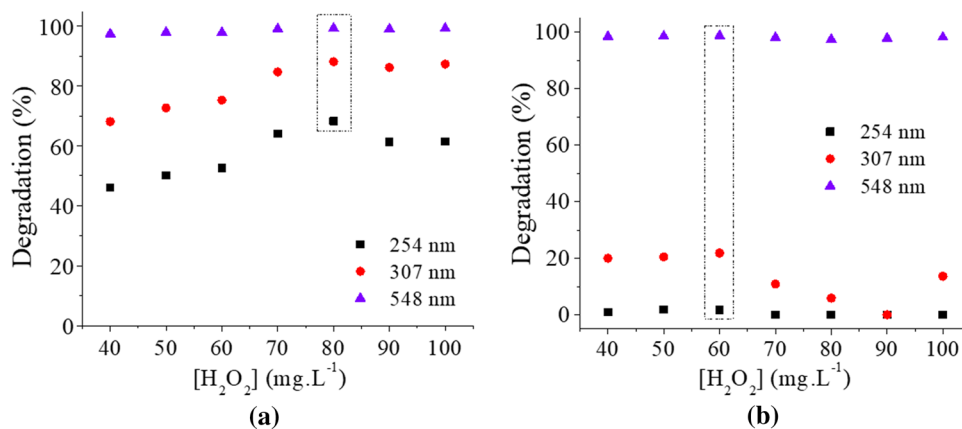
Thus, in general, the most efficient AOP for the degradation of the AV17 dye under the conditions employed was the photoperoxidation, using UV-C radiation. The photo-Fenton/UV-C treatment also showed good results, especially for the degradation of the chromophore group observed at 548 nm. However, as the color degradation was also satisfactory for the Fenton and photo-Fenton/sunlight processes and in view of the advantageous possibility of dispensing with the use of artificial radiation for the first case (it does not require radiation) and for the second case (the use of natural solar radiation, extremely available in northeastern Brazil), these AOP were selected for further studies. Thus, in the next step, the 3 processes, photoperoxidation, Fenton and photo-Fenton/sunlight, were evaluated to determine the best experimental conditions for treating the dye.

Optimization of the working conditions

For the photoperoxidation/UV-C and photo-Fenton/sunlight processes, a univariate study was carried out to determine the ideal $[H_2O_2]$ to be used in the AOP (Fig. 1).

As shown in Fig. 1a, the concentration that led to the highest percentage of degradation of AV17 through photoperoxidation/UV-C was 80 mg L^{-1}. In this case, the AOP led to degradation rates of 68.27%, 88.16% and 99.35% for the λ of 254, 307 and 548 nm, respectively. It is also possible to verify that from this amount of oxidizing agent, the degradation of AV17 became less efficient. As described by Martins et al. (2010), when present in excess, H$_2$O$_2$, acts as a scavenger of hydroxyl radicals, being, therefore, responsible for the reduction of the degradation percentages, as observed. Kumar et al. (2020) observed this same effect when evaluating the influence of $[H_2O_2]$ in the degradation of a mixture of dyes by the Fenton process under heterogeneous catalysis.

From Fig. 1b, it is possible to conclude that the limiting value of $[H_2O_2]$ in the photo-Fenton/sunlight process is 60 mg L^{-1}. In these conditions, the AOP promoted a degradation of 1.67%, 21.82% and 98.75% for the λ of: 254, 307 and 548 nm. However, the percentages obtained for this concentration did not show significant differences when compared to those obtained for the concentrations of 40 and 50 mg L^{-1}. For a $[H_2O_2] = 40$ mg L^{-1}, the degradation percentages obtained were 0.93%, 20% and 98.41%, for the respective λ. Therefore, the lower concentration of oxidizing agent was chosen for further studies, to reduce the costs associated with the process.

For the photo-Fenton/sunlight AOP, an additional study was carried out to compare the performance of the process when employing natural solar radiation. For this, the best working conditions defined for the sunlight radiation were adopted ([Fe] = 5 mg L^{-1} and $[H_2O_2] = 40$ mg L^{-1}). The experiment was carried out from 11 am to 12 pm, with a photon emission range of $4.08\cdot10^2$ to $1.65\cdot10^5$ W·m^{-2}. The degradation percentages obtained for both types of radiation are shown in Fig. 2.

As already observed in the preliminary study, different percentages of degradation were obtained for each characteristic wavelength, with a greater decrease in concentration
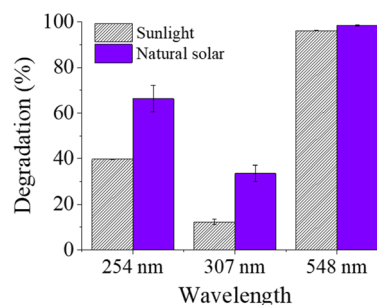
Fig. 2 Percentage of degradation of the dye AV17 observed for the photo-Fenton process, comparing the use of sunlight and natural solar radiation

Fig. 1 Univariate study of the $[H_2O_2]$ used in the AOP: **a** photoperoxidation/UV-C, **b** photo-Fenton/sunlight

observed for the chromophore group (548 nm). However, Fig. 2 shows that the use of natural solar radiation, when compared to artificial sunlight radiation, in the treatment via photo-Fenton led to higher degradation rates for all these λ. Thus, it becomes advantageous to substitute the use of artificial radiation for natural, especially in view of the high availability of this source in Northeast Brazil, where the experiments were carried out. The energy cost associated with the operation of the bench reaction equipped with sunlight radiation, in addition to the cost related to the design and construction of the reactor, whose lamp costs about $59,63 (Osram, 300 W), make the treatment process more costly when compared to the use of natural solar radiation.

As defined by *Companhia Elétrica de Pernambuco* (CELPE 2019), the average cost of kW·h is $0.136 for units belonging to the B3 group, as in the case of the Federal University of Pernambuco. Thus, the energy cost associated with the sunlight reactor is $0.0408·h^{-1}, for a reactor whose dimensions allow the degradation of a maximum of 1 L per residence time. As for the reactor equipped with UV-C radiation, used in the photoperoxidation AOP, this expenditure is about $0.012·h^{-1}, while the cost associated with obtaining the radiation source is around $57.90 (3 lamps, Phillips, 30 W). Therefore, natural solar radiation was used for the photo-Fenton treatment in the later stages.

It is worth noting that the pH adopted for the process was maintained in the 3–4 range as defined preliminary, this range being considered the ideal pH of the Fenton reaction (Lastre-Acosta et al. 2019). In addition, as reported by Babuponnusami and Muthukumar (2013), at a higher pH there is less availability of the free ferrous ions to catalyze the formation of oxidizing radicals, due to ferric hydroxide precipitation, in addition to the formation of iron oxyhydrates. These constitute a less active form of the catalyst, thus resulting in a decrease in the efficiency of the treatment.

For the Fenton AOP, the multivariate study of the parameters of greatest influence in the process (pH, [Fe] and [H$_2$O$_2$]) led to the construction of a Pareto chart (Fig. 3a). The observation of a significant influence of the interaction effects between pH and [Fe] was interpreted according to the surface graph obtained statistically (Fig. 3b). It is worth noting that the FD 2^3 with a central point was performed by the exclusive monitoring of the degradation of the chromophore groups (548 nm).

Figure 3a shows that the main effects [Fe] and pH and the interaction of these variables proved to be statistically significant for 95% confidence. It is also observed through the analysis of Fig. 4b that the increase in the values of these variables together results in higher percentages of degradation. The statistical evaluation also allows to affirm that the pH adopted for the treatment of the AV17 dye solution may be the closest to the natural pH of the working solution (pH 4), without reducing the efficiency of the treatment. This has the advantage of lesser use of reagents, as well as a more suitable condition for disposal in aquatic bodies. Thus, the best operating conditions for degradation of the AV17 chromophore group by the Fenton process are [H$_2$O$_2$] = 40 mg L^{-1}, [Fe] = 5 mg L^{-1} and pH 4, that promoted a color decay of 98.89%.

Having the best operating conditions for each of the three AOP evaluated, it was possible to define the cost associated with the reagents used to treat the solution contaminated by the dye. For the AOP that use Fenton's reagent, this value is about $0.77 per m^3 of treated solution. As for the photoperoxidation, the cost associated with the use of the oxidizing
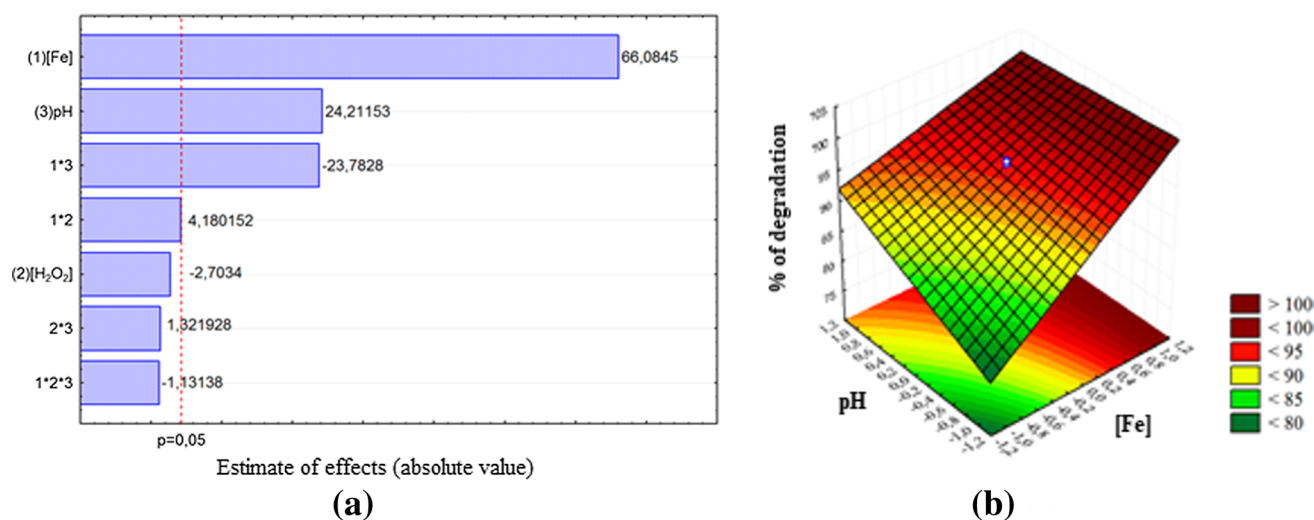

Fig. 3 Statistical analysis of the degradation of AV17 by the Fenton Process (λ = 548 nm): **a** Pareto Chart, **b** response surface interaction pH vs [Fe]

agent is \$0.95 per m^3 of treated solution, higher than the other processes, since it required a greater concentration of hydrogen peroxide.

Kinetic study of the degradation of the dye AV17 through different types of AOP

For the photoperoxidation/UV-C AOP, the kinetic study was performed with monitoring of all characteristic λ. The experimental data were first adjusted according to the first and second order models (Fig. 4).

Figure 4 shows that the second order model better represented the reaction kinetics when compared to the first order model, since it presented the highest linear regression coefficients (R^2). Santana et al. (2019b), when evaluating the degradation kinetics of dyes by the Fenton process, also observed that the degradation reactions were better described by the second order model. Figure 4b shows that the model described the degradation kinetics of the auxochromic groups observed at 254 nm, with R^2 > 0.99. For the discoloration kinetics, (in λ = 548 nm), none of the models presented good linearity. In addition to these, the nonlinear model of pseudo-first order was also tested for kinetic study of the degradation of the dye AV17 (Fig. 5).

As shown in Fig. 5, the degradation kinetics of the AV17 by the photoperoxidation/UV-C adjusted to the proposed model, with a regression coefficient (R^2) > 0.90 for all cases. It appears that this model better represents the decay of the concentration of the dye in relation to the linear models previously presented. The kinetics parameters of the model, $\frac{1}{\rho}$ and $\frac{1}{\sigma}$, represent the reaction kinetics and oxidative capacity of the system, allowing to estimate the initial decay rate observed in the monitored λ. Knowing this, it can be said that the discoloration kinetics, evaluated through λ = 548 nm, presented a faster trend than the degradation of the compounds associated with the other λ.

A similar result was obtained by Santana et al. (2019a, b) when studying the degradation of textile dyes using AOP. In this study, it was observed that the concentration decay observed in the chromophore group occurred more quickly than for the λ that represent auxochromes or aromatics groups present in the dye mixture.

For the Fenton and photo-Fenton/Solar processes, the kinetic study was also carried out, with the aforementioned models being tested. The decay of the concentration of the chromophore group for the Fenton and photo-Fenton processes is shown in Figs. 6 and 7, respectively.

By analyzing Figs. 6 and 7, it is verified again that the pseudo-first order model is the one that best describes the reaction kinetics, presenting $R^2 > 0.90$ for both AOP. None of the linear models presented a good fit to the experimental data. Regarding the processes presented, Fenton led to a much slower degradation of the chromophore group (observed at λ = 548 nm), with a rate of speed (1/ρ) lower than that observed for the photo-Fenton/solar. Through this process, the chromophore group underwent almost complete degradation in the first reaction minutes, similarly to what was observed for the treatment by the photoperoxidation using UV-C radiation.

At the end of the kinetic study, an additional test was performed to determine the residual concentration of the oxidizing agent after treatment via photoperoxidation/UV-C, Fenton and photo-Fenton/solar. The residual [H$_2$O$_2$] obtained were in the ranges of 0.5 mg L^{-1} to 2 mg L^{-1} (photoperoxidation/UV-C), 2 mg L^{-1} to 5 mg L^{-1} (Fenton) and 0 to 0.5 mg L^{-1-} (photo-Fenton/solar). This shows that the [H$_2$O$_2$] used largely consumed over the 120 min reaction, for each AOP studied. The presence of these quantities at the end of the process also indicates that the degradation reaction was not interrupted by the total consumption of the oxidizing agent.

Fig. 4 Degradation kinetics of AV17 by photoperoxidation/UV-C according to models of: **a** first order, **b** second order
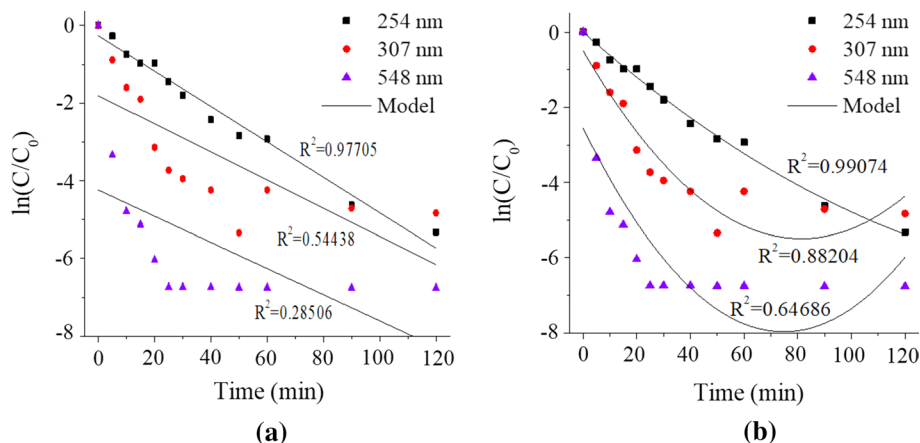
Fig. 5 Degradation kinetics of the AV17 by the photoperoxidation/UV-C process according to the pseudo-first order model, for **a** 254 nm, **b** 307 nm, and **c** 548 nm
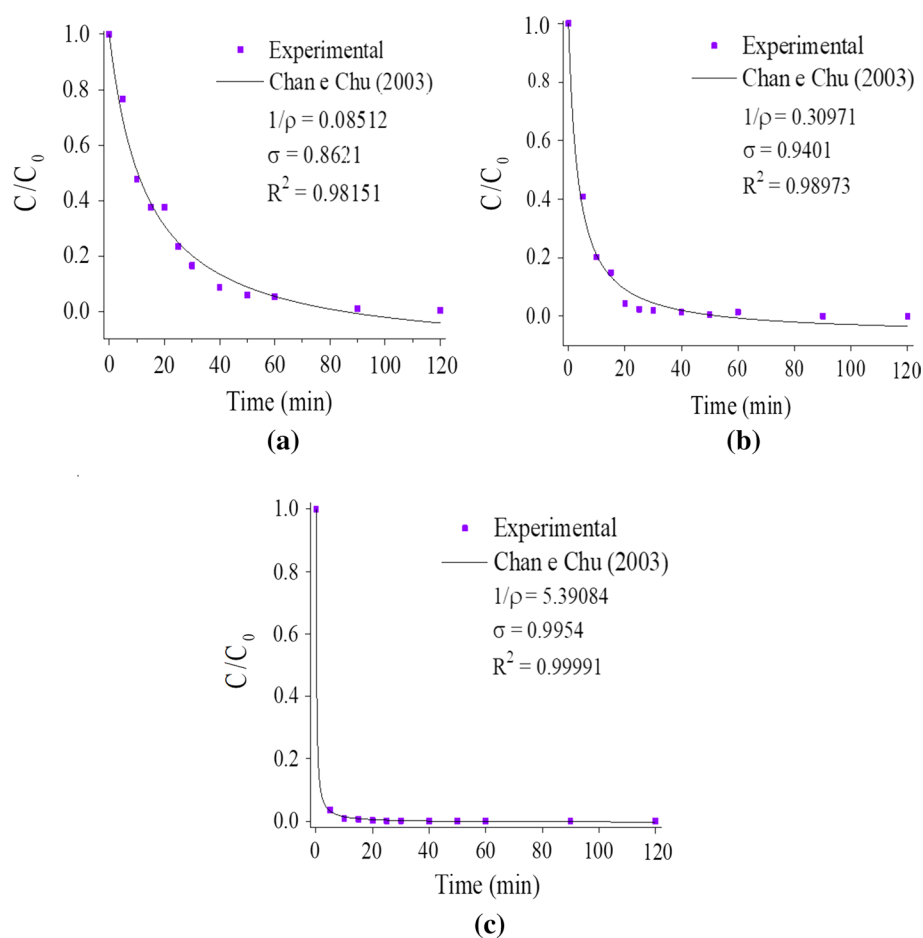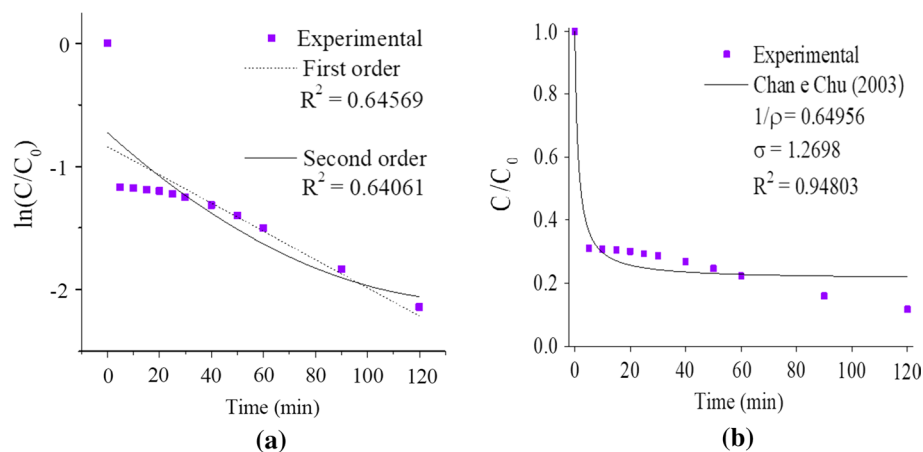

Fig. 6 Kinetics of the AV17 discoloration reaction via the Fenton process with adjustment to the models of: **a** first and second order, **b** pseudo-first order proposed by Chan and Chu (2003)

Artificial neural network modeling

Since a good degradation of the dye AV17 was verified in relation to the different AOP, a mathematical evaluation was carried out using artificial neural network (ANN). In this study, data from the Fenton, photo-Fenton and photoperoxidation processes were included. For this, when the treatment did not use any variable, a value of 0 was

assigned, such as, for example, the emission of photons = 0 for the Fenton AOP. The descriptive statistics of the five variables used in ANN are contained in Table 2.

Through the analysis of Table 2, it was possible to predict a degradation of the group referring to 254 nm equal to 99.51%. For the λ of 307 and 548 nm, the ANN shows that it is possible to obtain a degradation of 100% of these groups.

Optimizing the ANN topology is probably the most important step in model development. In the present work, a three-layer posterior propagation neural network (5-6-3) was used to model the degradation of the dye AV17, in its characteristic λ (254, 307 and 548 nm). In Fig. 8, the

diagram of the ANN MLP 5-6-3 BFGS 297 architecture can be observed, which presented better adequacy, managing to represent the treatment employed with greater reliability.

In Fig. 8, it is possible to observe that the training algorithm BFGS 297, with SOS error function, presented the

Fig. 7 Kinetics of the AV17 discoloration reaction via the natural photo-Fenton/solar process, with adjustment to the models of: **a** first and second order, **c** pseudo-first order proposed by Chan and Chu (2003)
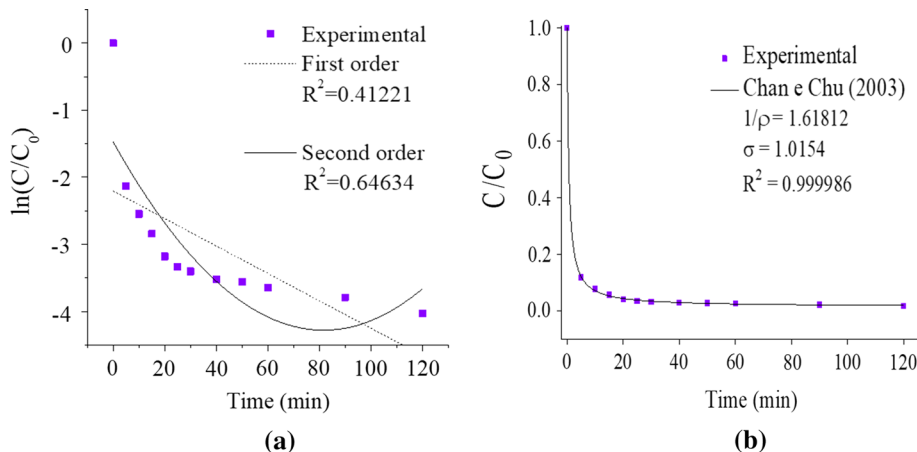
Table 2 Descriptive statistics of the variables used in ANN

Variables/samples	[Fe] (mg L^{-1})	pH	H$_2$O$_2$ (mg L^{-1})	Time (min)	Photon emission W/cm^{-2}	Degradation %		
						(254 nm)	(307 nm)	(548 nm)
Min (train)	0.00	2.00	40.00	5.00	0.00	0.00	0.00	68.90
Max (train)	5.00	5.50	120.00	120.0	13.81	**99.51**	**100.00**	**100.00**
Mean (train)	2.82	4.22	71.28	53.55	2.24	25.22	35.74	92.88
SD (train)	2.35	1.07	26.86	23.20	5.11	35.51	40.04	10.53
Min (test)	0.00	2.00	40.00	5.00	0.00	0.00	0.00	68.90
Max (test)	5.00	5.50	120.00	60.00	13.81	**94.63**	**98.56**	**100.00**
Mean (test)	2.54	4.15	63.33	40.00	3.45	35.00	42.18	90.49
SD (test)	2.40	1.22	22.78	20.43	6.11	38.64	42.15	12.18
Min (validation)	0.00	2.00	40.00	15.00	0.00	0.00	0.00	71.38
Max (validation)	5.00	5.50	120.00	120.0	13.81	**99.51**	**100.00**	**100.00**
Mean (validation)	2.83	4.33	71.67	62.71	4.60	27.95	41.13	95.41
SD (validation)	2.78	1.31	19.56	27.59	4.70	44.91	48.12	4.90

Fig. 8 Architecture diagram ANN MLP 5-6-3 BFGS 297
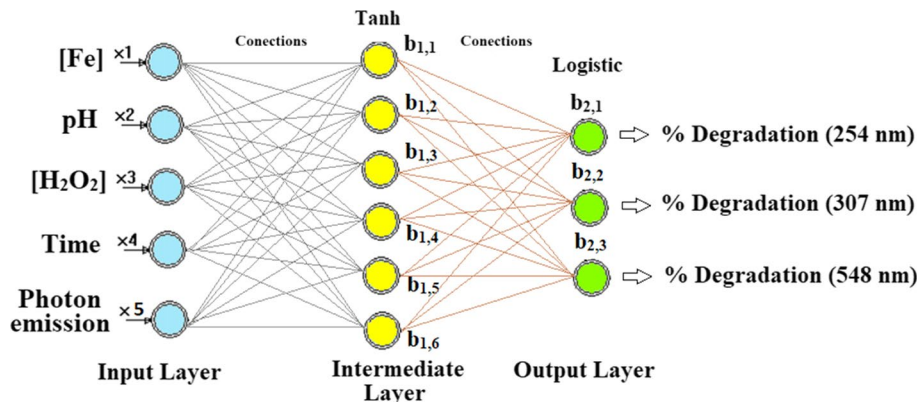
following activation functions: tanh for the internal layer and logistic for the output layer. This ANN, model (5-6-3), showed R^2 values equal to 0.9864; 0.9899 and 0.9894 for training, testing and validation, respectively.

To calculate training, validation and test errors, all outputs were performed on an inverse interval scale to return the predicted responses to their original scale. Then, they were compared with the experimental responses. The ANN used in this work provided the weights listed in Table 3.

The weights listed in Table 3 represent the coefficients between artificial neurons, which are analogous to the synapse strengths between axons and dendrites in real biological neurons. Therefore, each weight decided which proportion of the received signal will be transmitted to the neuron's body. Thus, it was possible to make comparisons between experimental and simulated MLP results (BFGS 297) for the studied wavelengths (Fig. 9).

Analyzing Fig. 9, it can be verified the good fit between experimental data and the simulated curve, indicating that the MLP ANN (BFGS 297) is able to reliably predict the degradation values for the λ studied. This result can be corroborated by the analysis of Fig. 10, which shows the linear regressions between the experimental and simulated results by the ANN.

From the analysis of Fig. 10, it appears that the MLP ANN (BFGS 297) was well suited for both the training stage, as well as the testing and validation stages. It is possible to say that the neural network model reproduces the degradation of compounds in this system, within the experimental ranges adopted in the assembly model. Likewise, other authors has also used ANN simulations to study treatments by AOP (Baştürk and Alver 2019, Zulfiqar et al. 2019, Nascimento et al. 2018, Eskandarloo et al. 2016). Monteiro et al. (2018), when evaluating the degradation of the drugs nimesulide and ibuprofen by the photo-Fenton process, managed to predict, using an MLP ANN (BFGS 4567), the TOC conversion of the mixture,

demonstrating once again the ability of this type of modeling to predict the degradation data via AOP.

Seed toxicity tests

From the toxicity tests with lettuce seeds (*Lactuca sativa*) it was possible to determine the relative growth (RGI) and germination (GI) indexes for the solutions before treatment (SBT), and the solutions treated via AOP: photoperoxidation/UV-C (SPT PP), Fenton (SPT F) and photo-Fenton/natural solar (SPT PF). The results obtained are shown in Fig. 11.

As shown in Fig. 11, the RGI and GI values for the pre and post-treatment solutions via the Fenton processes were significantly lower than that presented by the negative control. This is indicative of the toxic potential of the dye solution before being treated, and of the possible formation of toxic intermediates after the treatment with the Fenton process. In addition, the presence of residual hydrogen peroxide with a concentration in the rage of 2 to 5 mg.L^{-1} in the solution treated by the Fenton process may have contributes to promote the inhibition of seed development.

The photoperoxidation/UV-C and photo-Fenton/solar AOP showed an increase in both RGI and GI in relation to the initial solution, with RGI values > 0.80, which indicates that there was no inhibition of relative seed growth (Young et al. 2012). For the photo-Fenton process, both RGI and GI were shown to be superior to the negative control performed, indicating that there was growth stimulation according to these same authors.

Conclusions

The application of advanced oxidation processes promoted the efficient degradation of the acid violet 17 dye. The photoperoxidation/UV-C process led to the best degradation

Table 3 Weights values for the input, intermediate and output layers of the ANN MLP 5-6-3 (BFGS 297, Tanh- Logistic)

| Neuron	Weights								
	$[Fe^{2+}]$ (mg L^{-1})	pH	$[H_2O_2]$ (mg L^{-1})	Time (min)	Photon emission	Bias input	Degradation % (254 nm)	Degradation % (307 nm)	Degradation % (548 nm)
1	− 42.1853	51.5751	− 49.2072	− 44.4721	− 4.2228	− 0.5510	1.0100	1.5753	0.3307
2	− 22.4839	− 26.287	0.1568	− 8.1308	− 0.3100	23.4745	− 39.9095	0.1031	− 1.5620
3	17.0337	− 2.5955	− 6.8351	37.6682	10.8232	− 11.771	− 1.1505	− 2.0819	− 0.9421
4	− 69.5493	− 12.324	13.0279	107.8239	− 7.9802	− 57.771	65.6201	54.3969	1.5943
5	− 3.9262	− 3.8445	1.1659	3.0529	15.0432	4.1199	11.1674	18.2971	9.2369
6	− 57.6254	− 1.0721	− 8.0871	68.1060	20.7035	8.1626	72.9851	1.1147	− 5.8984
Bias intermediates							− 57.7037	37.3478	0.4673
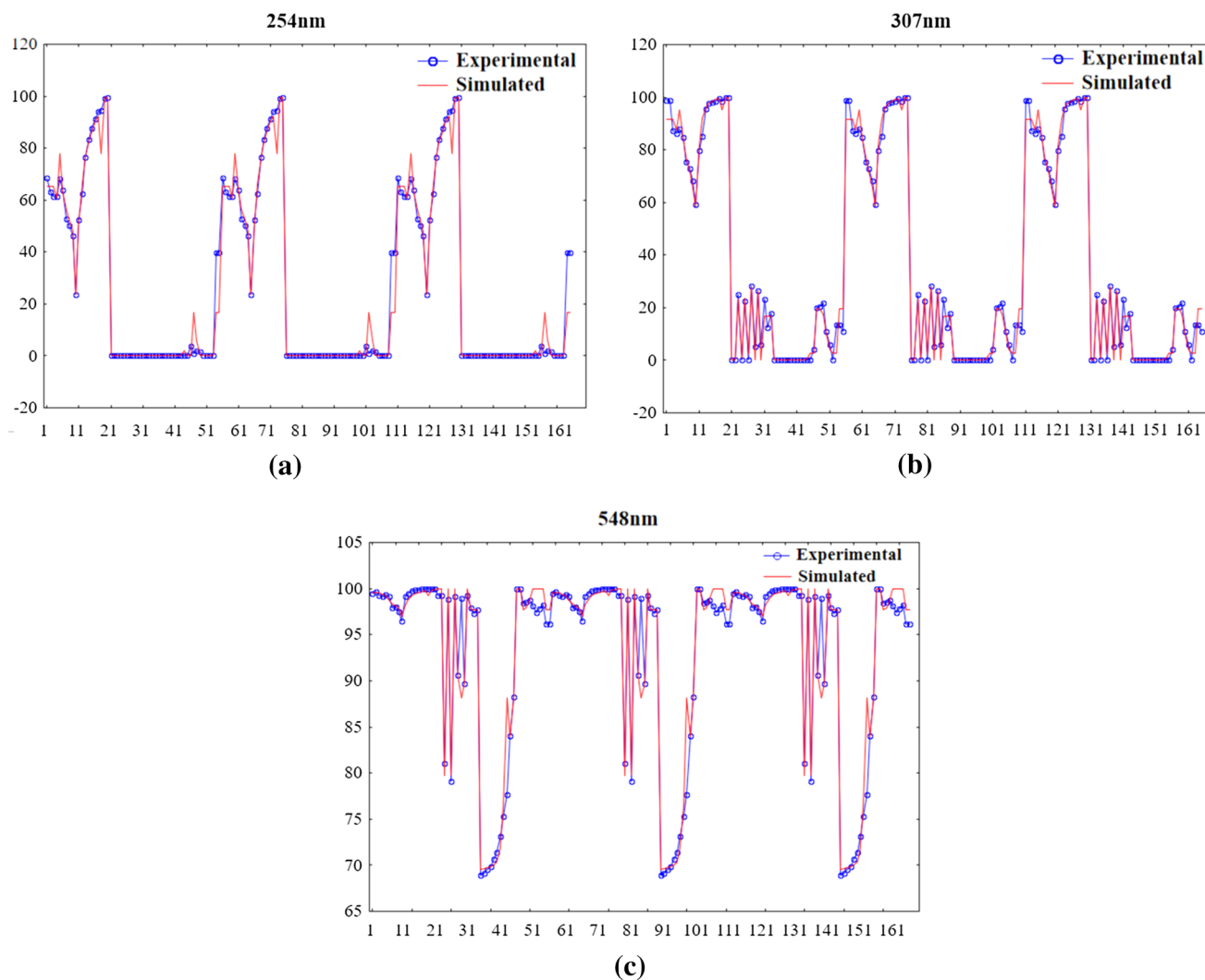
Fig. 9 Comparison between experimental and simulated MLP results (BFGS 297), for λ: **a** 254 nm, **b** 307 nm and **c** 548 nm

results, with a limiting concentration of $[H_2O_2] = 80$ mg L^{-1} and an efficiency higher than 68.27% being observed for the wavelengths analyzed. The Fenton and photo-Fenton AOP promoted good discoloration of the contaminated solution, with the following operational conditions being defined: $[Fe] = 5$ mg L^{-1}, $[H_2O_2] = 40$ mg L^{-1} and pH 4 for the Fenton process, and $[H_2O_2] = 40$ mg L^{-1}, $[Fe] = 5$ mg L^{-1} and pH 3–4 for the photo-Fenton/solar process. These treatments led to percentages of degradation of the chromophore group above 98%.

The three processes presented a reaction kinetics better represented by the nonlinear pseudo-first order model, with a $R^2 > 0.90$. The photoperoxidation/UV-C AOP led to a faster discoloration, followed by the photo-Fenton/solar treatment, while the Fenton process was slower. It was verified that an

ANN MLP (BFGS 297) was able to predict the degradation of the AV17 dye in its characteristic wavelengths by the studied treatments. As for the toxicological tests with *Lactuca sativa* seeds, the toxicity of the dye solution was reduced using the photoperoxidation/UV-C and photo-Fenton/natural solar processes. For the latter, stimulation of seed germination and growth was observed. While the Fenton process led to the formation of potentially toxic intermediates. In this case, future tests are necessary to identify and treat the intermediates by-products formed after the treatments, especially for the Fenton process. In addition, the efficiency evaluation of the treatment processes for effluents containing the AV17 dye, using the optimized operational variables, will guarantee the correct discharge of effluents in the environment.
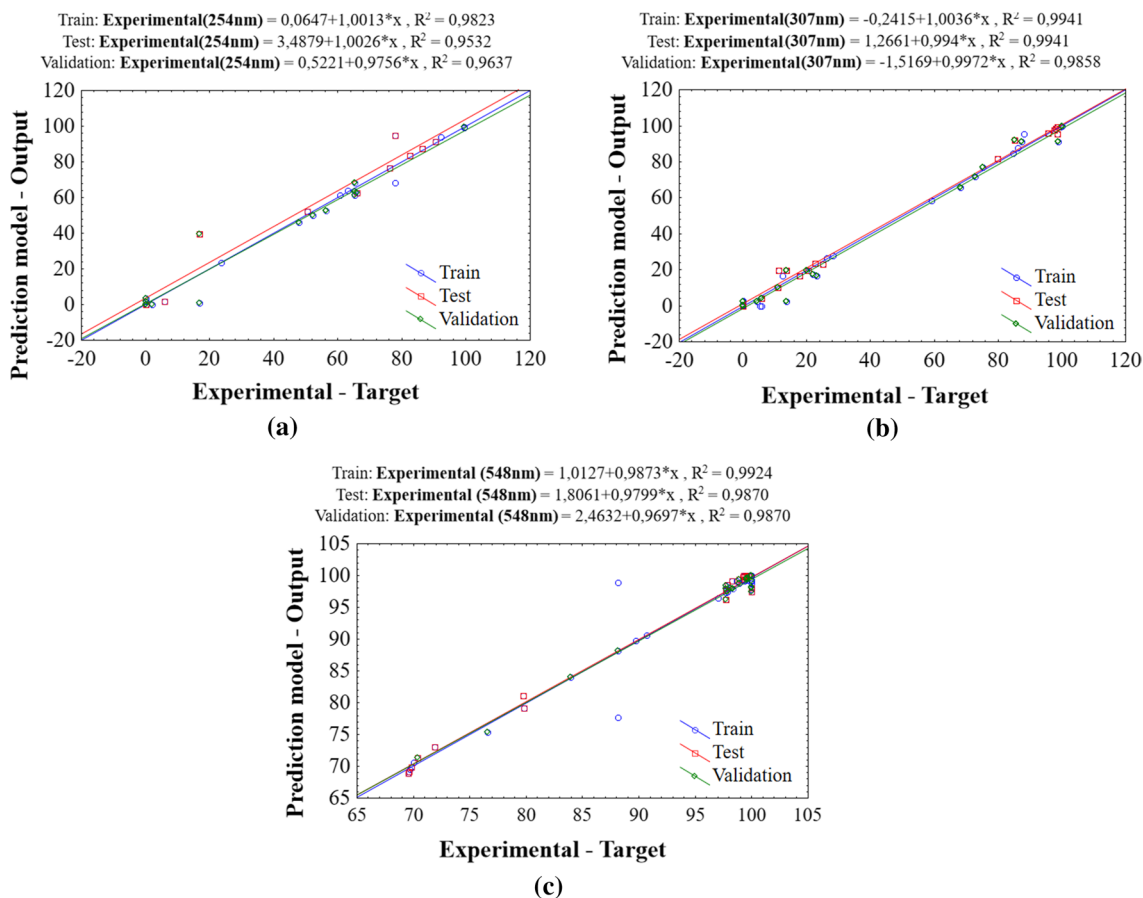
Train: **Experimental(254nm)** = 0,0647+1,0013*x , R^2 = 0,9823
Test: **Experimental(254nm)** = 3,4879+1,0026*x , R^2 = 0,9532
Validation: **Experimental(254nm)** = 0,5221+0,9756*x , R^2 = 0,9637

(a)

Train: **Experimental (307nm)** = −0,2415+1,0036*x , R^2 = 0,9941
Test: **Experimental(307nm)** = 1,2661+0,994*x , R^2 = 0,9941
Validation: **Experimental(307nm)** = −1,5169+0,9972*x , R^2 = 0,9858

(b)

Train: **Experimental (548nm)** = 1,0127+0,9873*x , R^2 = 0,9924
Test: **Experimental (548nm)** = 1,8061+0,9799*x , R^2 = 0,9870
Validation: **Experimental (548nm)** = 2,4632+0,9697*x , R^2 = 0,9870

(c)

Fig. 10 Linear regressions between the experimental and simulated results of the ANN MLP (BFGS 297) for λ: **a** 254 nm, **b** 307 nm and **c** 548 nm

Fig. 11 Ecotoxicity tests with *Lactuca sativa* seeds for the AV17 solution before and after treatment, showing: **a** RGI; **b** GI
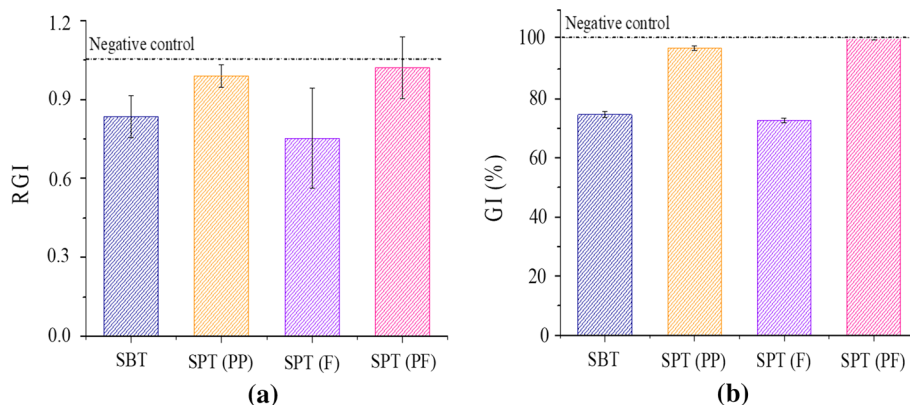
(a)　　**(b)**

References

Brasil. Anvisa. Agência Nacional de Vigilância Sanitária. Resolução da Diretoria Colegiada – RDC n. 321, 28 de novembro de 2019

Abid MF, Zablouk MA, Abid-Alameer AM (2012) Experimental study of dye removal from industrial wastewater by membrane

technologies of reverse osmosis and nanofiltration. J Environ Health Sci Eng 9(1):17. https://doi.org/10.1186/1735-2746-9-17

Abo-Farha SA (2010) Comparative study of oxidation of some azo dyes by different advanced oxidation processes: Fenton, Fenton-like, photo-Fenton and photo-Fenton-like. J Am Sci 6(10):128–142

Álvarez PM, Pocostales JP, Beltrán FJ (2011) Granular activated carbon promoted ozonation of a food-processing secondary effluent. J Hazard 185(2–3):776–783. https://doi.org/10.1016/j.jhazmat.2010.09.088

Araújo KS, Antonelli R, Gaydeczka B, Granato AC, Malpass GRP (2016) Processos oxidativos avançados: uma revisão de fundamentos e aplicações no tratamento de águas residuais urbanas e efluentes industriais. Rev Ambient Água 11(2):387–401. https://doi.org/10.4136/ambi-agua.1862

Baştürk E, Alver A (2019) Modeling azo dye removal by sono-fenton processes using response surface methodology and artificial neural network approaches. J Environ Manage 248:109300. https://doi.org/10.1016/j.jenvman.2019.109300

Bousnoubra I, Djebbar K, Abdessemed A, Sehili T (2016) Decolorization of methyl green and bromocresol purple in mono and binary systems by photochemical processes: direct UV photolysis, Acetone/UV and H_2O_2/UV. A comparative study. Desalin Water Treat 57(57):27710–27725. https://doi.org/10.1080/19443994.2016.1174741

Brillas E (2020) A review on the photoelectro-Fenton process as efficient electrochemical advanced oxidation for wastewater remediation. Treatment with UV light, sunlight, and coupling with conventional and other photo-assisted advanced technologies. Chemosphere 250:126198. https://doi.org/10.1016/j.chemosphere.2020.126198

Chan KH, Chu W (2003) Modeling the reaction kinetics of Fenton's process on the removal of atrazine. Chemosphere 51(4):305–311. https://doi.org/10.1016/s0045-6535(02)00812-3

Charamba LVC, Santana RMR, Nascimento GE, Charamba BVC, Moura MC, Coelho LCBB, Napoleão DC (2018) Application of the advanced oxidative process on the degradation of the green leaf and purple açaí food dyes with kinetic monitoring and artificial neural network modelling. Water Sci Technol 78(5):1094–1103. https://doi.org/10.2166/wst.2018.391

Companhia Energética De Pernambuco—CELPE(2019) Tabela de Tarifas de Energia Elétrica. Grupo B. Resolução homologatória No 2535 de 25 de abril de 2019. Vigência: 29/04/2019 a 28/04/2020

Brasil. Anvisa. Agência Nacional de Vigilância Sanitária. Resolução n. 899, de 29 de maio de 2003. Guia para validação de métodos analíticos e bioanalíticos

Deshannavar UB, Singa PK, Gaonkar D, Gayathri A, Patil A, Malade LV (2020) Removal of acid violet 49 and acid red 88 dyes from aqueous solutions using advanced oxidation process. Mater Today Proc 24:1011–1019. https://doi.org/10.1016/j.matpr.2020.04.414

Elkacmi R, Bennajah M (2019) Advanced oxidation technologies for the treatment and detoxification of olive mill wastewater: a general review. Water Reuse Desal 9(4):463–505. https://doi.org/10.2166/wrd.2019.033

Ertugay N, Acar FN (2017) Removal of COD and color from Direct Blue 71 azo dye wastewater by Fenton's oxidation: kinetic study. Arab J Chem 10:S1158–S1163. https://doi.org/10.1016/j.arabjc.2013.02.009

Eskandarloo H, Badiei A, Behnajady MA, Ziarani GM (2016) Hybrid homogeneous and heterogeneous photocatalytic processes for removal of triphenylmethane dyes: artificial neural network modeling. Clean: Soil, Air, Water 44(7):739–908. https://doi.org/10.1002/clen.201400449

Fernandes NC, Brito LB, Costa GG, Taveira SF, Cunha-Filho MSS, Oliveira GAR, Marreto RN (2018) Removal of azo dye using Fenton and Fenton-like processes: evaluation of process factors by Box-Behnken design and ecotoxicity tests. Chem Biol Interact 291:47–54. https://doi.org/10.1016/j.cbi.2018.06.003

Ferrando-Climent L, Gonzalez-Olmos R, Anfruns A, Aymerich I, Corominas L, Barceló D, Rodriguez-Mozaz S (2017) Elimination study of the chemotherapy drug tamoxifen by different advanced oxidation processes: transformation products and toxicity assessment. Chemosphere 168:284–292. https://doi.org/10.1016/j.chemosphere.2016.10.057

Golka K, Kopps S, Myslak ZW (2004) Carcinogenicity of azo colorants: influence of solubility and bioavailability. Toxicol Lett 151(1):203–210. https://doi.org/10.1016/j.toxlet.2003.11.016

Instituto Nacional de Metrologia, Normalização e Qualidade Industrial – INMETRO (2016) DOC-CGCRE-008: Orientação sob validação de métodos analíticos

Jain SN, Gogate PR (2017) Adsorptive removal of acid violet 17 dye from wastewater using biosorbent obtained from NaOH and H_2SO_4 activation of fallen leaves of Ficusracemosa. J Mol Liq 243:132–143. https://doi.org/10.1016/j.molliq.2017.08.009

Júnior WDN, Aquino RVS, Barbosa AA, Rocha OR (2019) Development of a new PET flow reactor applied to food dyes removal with advanced oxidative processes. J Water Process Eng 31:100823. https://doi.org/10.1016/j.jwpe.2019.100823

Korpe S, Bethi B, Sonawane SH, Jayakumar KV (2019) Tannery wastewater treatment by cavitation combined with advanced oxidation process (AOP). Ultrason Sonochem 59:104723. https://doi.org/10.1016/j.ultsonch.2019.104723

Kumar V, Ghime D, Ghosh P (2019) Decolorization of textile dye Rifafix Red 3BN by natural hematite and a comparative study on different types of Fenton process. Chem Eng Commun. https://doi.org/10.1080/00986445.2019.1652603

Kumar V, Pandey N, Dharmadhikari S, Ghosh P (2020a) Degradation of mixed dye via heterogeneous Fenton process: studies of calcination, toxicity evaluation, and kinetics. Water Environ Res 92(2):211–221. https://doi.org/10.1002/wer.1192

Kumar JE, Mulai T, Kharmawphlang W, Sharan RN, Sahoo MK (2020b) Decolourisation, mineralisation and detoxification of mixture of azo dyes using Fenton and Fenton-type advanced oxidation processes. Chem Pap. https://doi.org/10.1007/s11696-020-01147-9

Lastre-Acosta AM, Vicente R, Mora M, Jáuregui-Haza UJ, Arques A, Teixeira ACSC (2019) Photo-Fenton reaction at mildly acidic conditions: assessing the effect of bio-organic substances of different origin and characteristics through experimental design. J Environ Sci Heal A 54(8):711–720. https://doi.org/10.1080/10934529.2019.1585721

Martins RC, Rossi AF, Quinta-Ferreira RM (2010) Fenton's oxidation process for phenolic wastewater remediation and biodegradability enhancement. J Hazard Mater 180(1–3):716–721. https://doi.org/10.1016/j.jhazmat.2010.04.098

Monteiro RT, Santana RMR, Silva AMRB, Lucena ALA, Zaidan LEMC, Silva VL, Napoleão DC (2018) Degradation of the pharmaceuticals nimesulide and ibuprofen using photo-Fenton process: toxicity studies, kinetic modeling and use of artificial neural networks. Rev Eletrônica Gest Educ Tecnol Ambient 22:3. https://doi.org/10.5902/2236117031563

Nascimento GE, Napoleão DC, Silva PKA, Santana RMR, Bastos AMR, Zaidan LEMC, Duarte MMMB (2018) Photo-assisted degradation, toxicological assessment, and modeling using artificial neural networks of reactive gray BF-2R dye. Water Air Soil Pollut 229(12):379. https://doi.org/10.1007/s11270-018-4028-2

Navarro P, Gabaldón JA, Gómez-López VM (2017) Degradation of an azo dye by a fast and innovative pulsed light/H2O2 advanced oxidation process. Dyes Pigm 136:887–892. https://doi.org/10.1016/j.dyepig.2016.09.053

Pavithra KG, Jaikumar V (2019) Removal of colorants from wastewater: a review on sources and treatment strategies. J Ind Eng Chem 75:1–19. https://doi.org/10.1016/j.jiec.2019.02.011

Paździor K, Bilińska L, Ledakowicz S (2019) A review of the existing and emerging technologies in the combination of AOPs and biological processes in industrial textile wastewater treatment. Chem Eng J 376:120597. https://doi.org/10.1016/j.cej.2018.12.057

Ramos RO, Albuquerque MV, Lopes WS, Sousa JT, Leite VD (2020) Degradation of indigo carmine by photo-Fenton, Fenton, H_2O_2/UV-C and direct UV-C: comparison of pathways, products and kinetics. J Water Process Eng 37:101535. https://doi.org/10.1016/j.jwpe.2020.101535

Santana RMR, Nascimento GE, Napoleão DC, Duarte MMMB (2017) Degradation and kinetic study of Reactive blue BF-5G and Remazol red RB 133% dyes using Fenton and photo-Fenton process. Rev Eletrônica Gest Educ Tecnol Ambient 21(2):104–118. https://doi.org/10.5902/2236117027358

Santana CS, Velloso CCV, Aguiar A (2019a) A kinetic study about the influence of phenolic mediators in the decolorization of different dyes by fenton systems. Quim Nova 42(2):149–155. https://doi.org/10.21577/0100-4042.20170316

Santana RMR, Charamba LCV, Nascimento GE, Oliveira JGC, Sales DCS, DuarteMMMB Napoleão DC (2019b) Degradation of textile dyes employing advanced oxidative processes: kinetic, equilibrium modeling, and toxicity study of seeds and bacteria. Water Air Soil Pollut 230(6):136. https://doi.org/10.1007/s11270-019-4178-x

Santos MMM, Duarte MMMB, Nascimento GE, Souza NBGD, Rocha ORSD (2019) Use of TiO_2 photocatalyst supported on residues of polystyrene packaging and its applicability on the removal of food dyes. Environ Technol 40(12):1494–1507. https://doi.org/10.1080/09593330.2017.1423396

Shemer H, Kunukcu YK, Linden KG (2006) Degradation of the pharmaceutical metronidazole via UV. Fenton and photo-Fenton processes. Chemosphere 63(2):269–276. https://doi.org/10.1016/j.chemosphere.2005.07.029

Stalter D, Magdeburg A, Weil M, Knacker T, Oehlmann J (2010) Toxication or detoxication? In vivo toxicity assessment of ozonation as advanced wastewater treatment with the rainbow trout. Water Res 44(2):439–448. https://doi.org/10.1016/j.watres.2009.07.025

Utzig LM, Lima RM, Gomes MF, Ramsdorf WA, Martins LR, Liz MV, Freitas AM (2019) Ecotoxicity response of chlorpyrifos in Aedes aegypti larvae and Lactuca sativa seeds after UV/H_2O_2 and UVC oxidation. Ecotoxicol Environ Safe 169:449–456. https://doi.org/10.1016/j.ecoenv.2018.11.003

Yaseen DA, Scholz M (2019) Textile dye wastewater characteristics and constituents of synthetic effluents: a critical review. Int J Environ Sci Technol 16(2):1193–1226. https://doi.org/10.1007/s13762-018-2130-z

Young BJ, Riera NI, Beily ME, Bres PA, Crespo DC, Ronco AE (2012) Toxicity of the effluent from an anaerobic bioreactor treating cereal residues on *Lactuca sativa*. Ecotoxicol Environ Saf 76:182–186. https://doi.org/10.1016/j.ecoenv.2011.09.019

Zaidan LEMC, Pinheiro RB, Santana RMR, Charamba LVC, Napoleão DC, Silva VL (2017) Evaluation of efficiency of advanced oxidative process in degradation of 2-4 dichlorophenol employing UV-C radiation reator. Rev Eletrôn Gest Educ Tecnol Ambient 21(2):147–157. https://doi.org/10.5902/2236117027766

Zulfiqar M, Samsudin MFR, Sufian S (2019) Modelling and optimization of photocatalytic degradation of phenol via TiO_2 nanoparticles: an insight into response surface methodology and artificial neural network. J Photochem Photobio A 384:112039. https://doi.org/10.1016/j.jphotochem.2019.112039

Publisher's Note Springer Nature remains neutral with regard to jurisdictional claims in published maps and institutional affiliations.